Name: Tung Yan YEUNG (mh23476)

COMSOL Assignment (Advanced Optoelectronic Devices)

This coursework answer is based on Professor's uploaded COMSOL file.

Task 1 (60%): Basic simulation setup

1.1 Vary the waveguide width between 200 nm and 1 um and plot the mode effective refractive index, n_{eff}(for both TE and TM).

- The n_{eff} against waveguide width for TE and TM modes are plotted in the graph.
- Between waveguide width 200nm and 1um, hybrid modes exist at inflection points, i.e. between TM0 and TE1, TE1 and TM0.
- Modes below 1.5 are crossed out as they are non-physical modes.

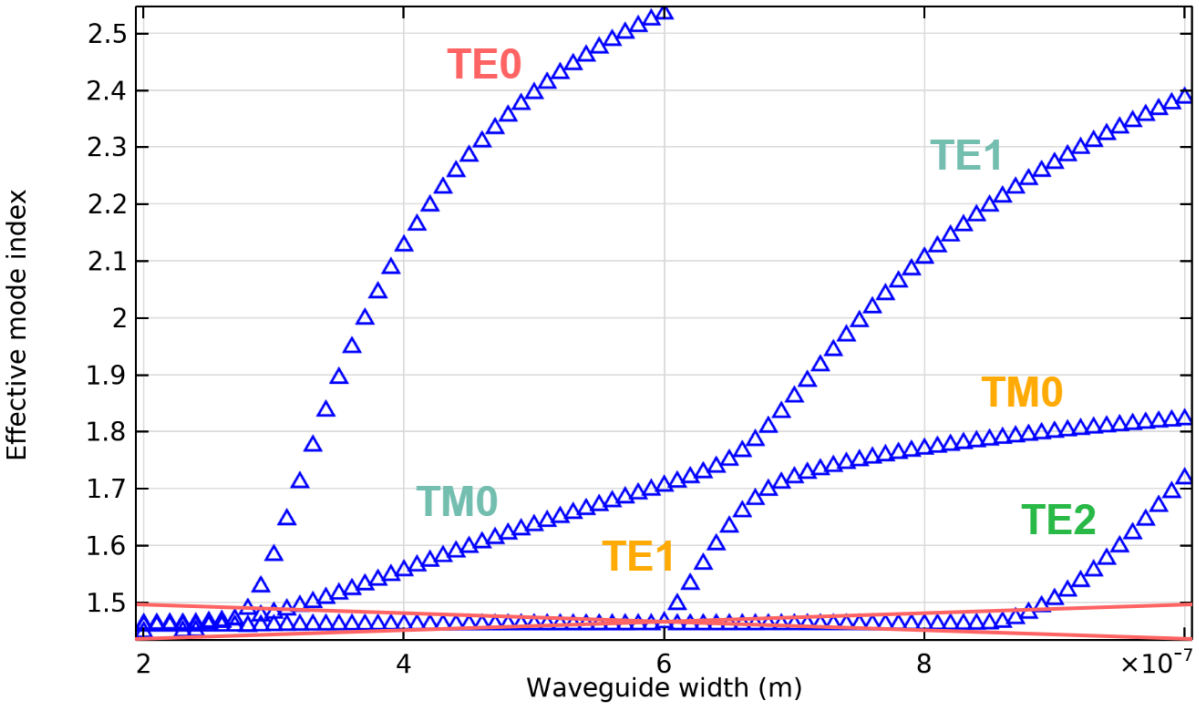

1.2 How do you tell the difference between TE and TM modes?

When Electric field of the incident EM wave is parallel to the plane of incidence it is called TE mode. And when Electric field is perpendicular to the plane of incidence, the wave is called TM mode.

I will show examples of the fundamental modes to explain. For plotting this field distribution, Ex component is selected to plot the TE polarisation and the Ey component is selected for the TM mode. This is identical with the explanation before.

The obtained abs(emw.Ex), i.e. $|E_x|$ component field profile of the fundamental TE in Fig 1(a) and abs(emw.Ey), i.e. $|E_y|$ component field profile of the fundamental TM in Fig 2(b) modes of 500nm waveguide clearly show that

- The fundamental TE mode is characterised by much higher field intensity at the side wall.
- The TM mode has much higher amplitude at the top and bottom interface.
- By looking at the n_{eff}, TE mode has a higher n_{eff} than TM mode.

In contrast, Fig 1(b) plots the Ey for TE and Fig 2(a) plots the Ex for TM in which there should not be electrical field intensity being observed inside the waveguide.

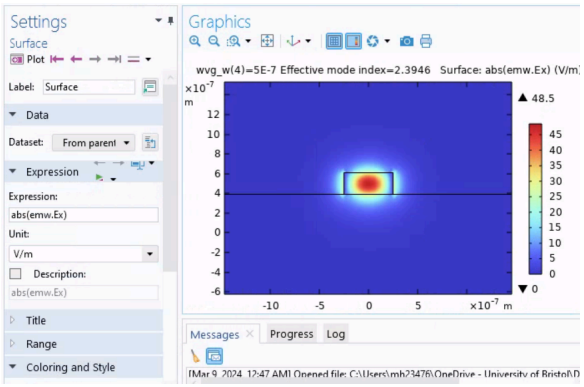

Fig 1(a)

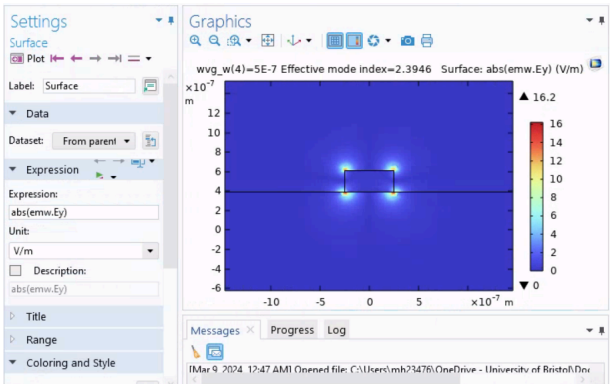

Fig 1(b)

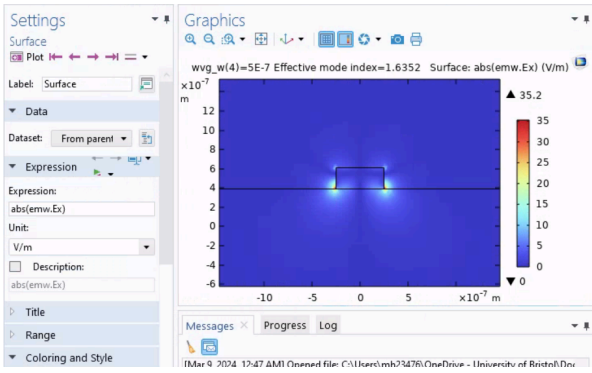

Fig 2(a)

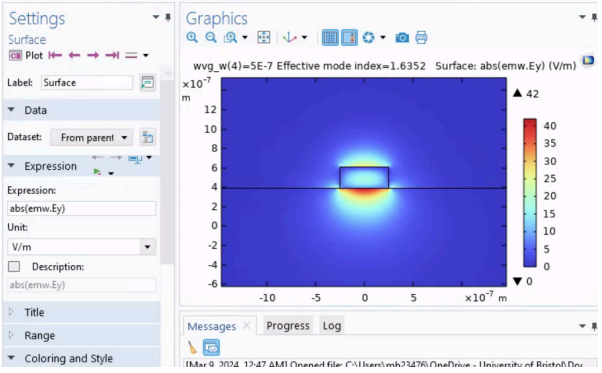

Fig 2(b)

Fig 1(a). Intensity profile of the electric field $|E_x|$ of TE mode. Fig 1(b). Intensity profile of the electric field $|E_y|$ of TE mode. Fig 2(a). Intensity profile of the electric field $|E_x|$ of TM mode. Fig 2(b). Intensity profile of the electric field $|E_y|$ of TM mode.

1.3 At what width does the waveguide become multi-moded? Note: here the second mode we are interested in is the higher order TE mode.

The emw.normE or abs(emw.Ex) could distinguish between single mode and multi-moded. However, in this question, emw.Ex is being used to distinguish them for easier observation.

Fig 3(a) plots the Ex component of the waveguide at 600nm, compared to Fig 3(b) Ex component of the waveguide at 610nm started to split into two intensity sources. It is observed that the waveguide started to form a multimode since 610nm. Until 690nm, the multi-moded waveguide is formed completely as TE1 since no intensity can be observed within the boundary of the waveguide in the Ey component as shown in Fig 4(a). Ex component of the complete formed multi-moded waveguide is plotted in Fig 4(b).

In short, at 610nm, the waveguide started becoming multi-moded.

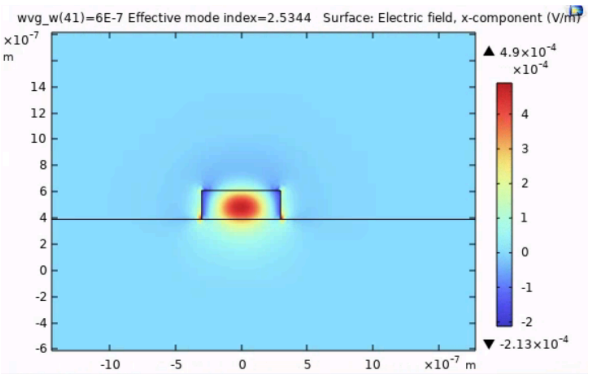

Fig 3(a)

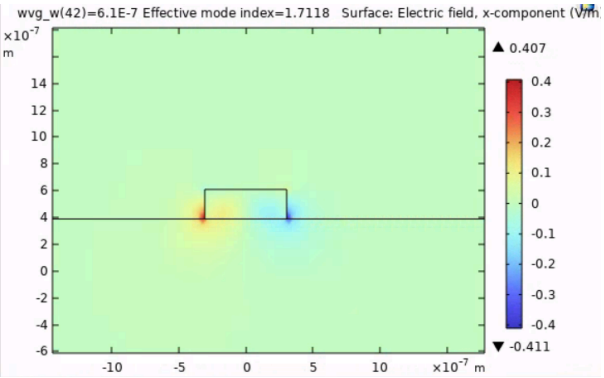

Fig 3(b)

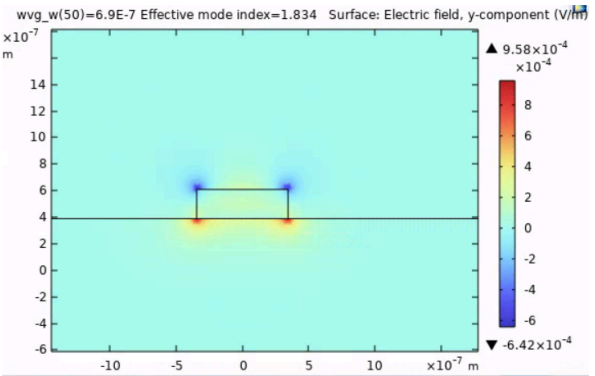

Fig 4(a)

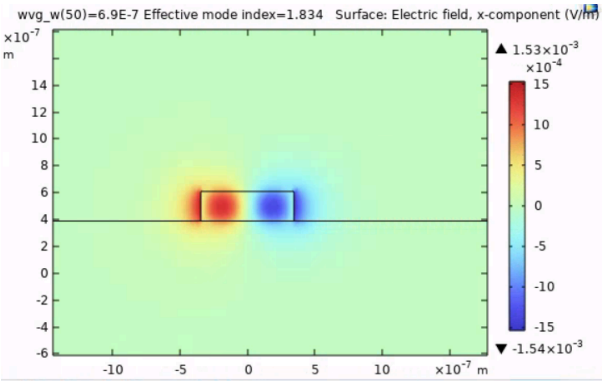

Fig 4(b)

Fig 3(a). E_X of TE0 at 600nm. Fig 3(b). E_x of TE1 at 610nm. Fig 4(a). E_y of TE1 at 690nm. Fig 4(b). E_x of TE1 at 690nm.

1.4 Change the top cladding to oxide, how does this change the width at which the waveguide becomes multi-moded?

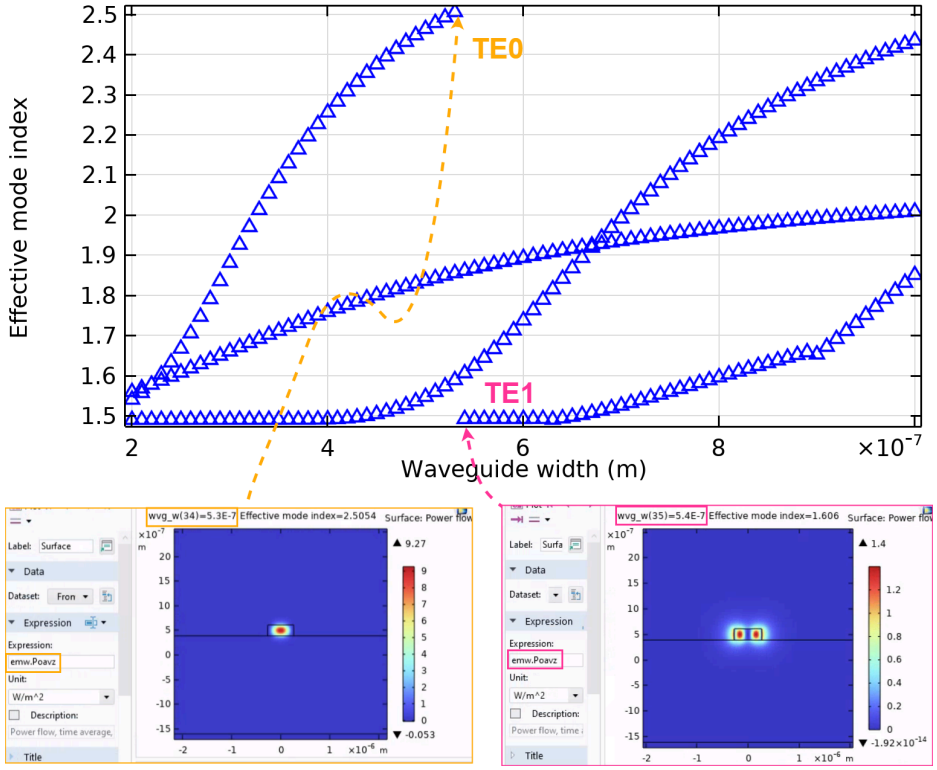

When the top cladding is changed from air to oxide, from the plot, it is observed that the waveguide becomes multi-moded at 540nm, it means the waveguide becomes multi-moded with a shorter waveguide width. Apart from using the method in Q1.3 (i.e. abs(emw.Ex)) to identify single mode and multi-moded, we can also use average power flow.

For example, to verify the observation multi-moded starts at 540nm, average power that is perpendicular to z (i.e. emw.povaz) is used to identify a point in TE0 that only gives one intensity source and the first point at TE1. The waveguide at 540nm is proved to have two sources plotted in average power.

Task 2 (40%): Dispersion calculation on and four wave mixing (FWM)

For task 2, we will keep the silicon waveguide's width fixed at 500 nm and plot the mode effective refractive index for the fundamental TE mode as a function of wavelength (1.2-1.8 μm)

2.1 Assume silicon's refractive index varies according to the Sellmeier equation for the mode effective refractive index calculation:

$$n_{si}^2(\lambda) = 1 + \frac{10.6684293\ \lambda^2}{\lambda^2 - 0.30151685^2} + \frac{0.0030434748\ \lambda^2}{\lambda^2 - 1.13475115^2} + \frac{1.54133408\ \lambda^2}{\lambda^2 - 1104^2}$$

Cladding is changed back to air for Task 2.

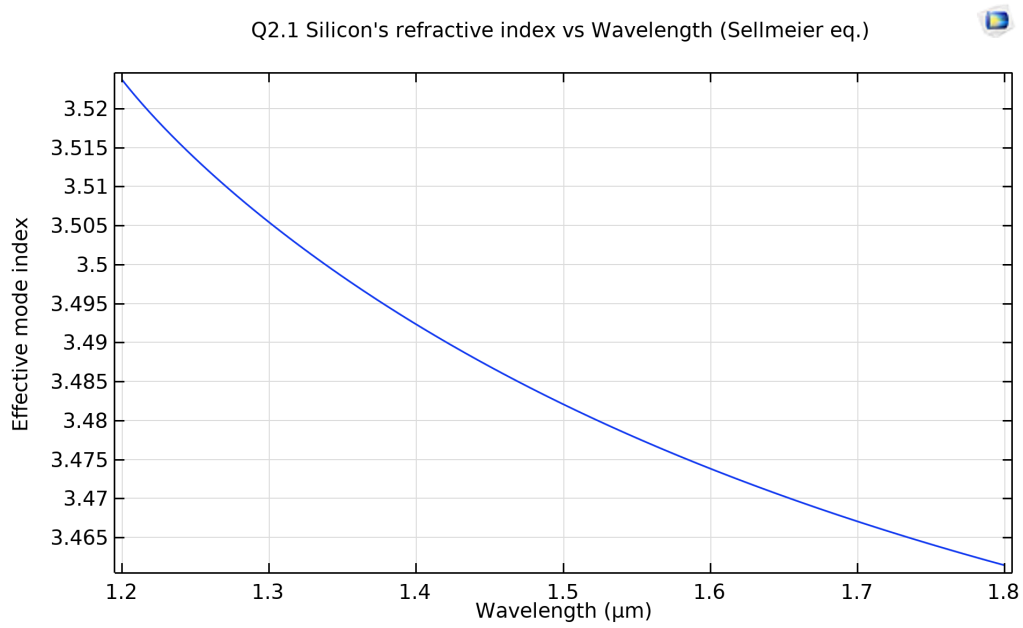

2.2 Calculate $\frac{dn}{d\lambda}$ and $\frac{d^2n}{d\lambda^2}$ for the material index. (Hint: numerical derivatives are fine, no need to do this analytically. Wavelength is in microns)

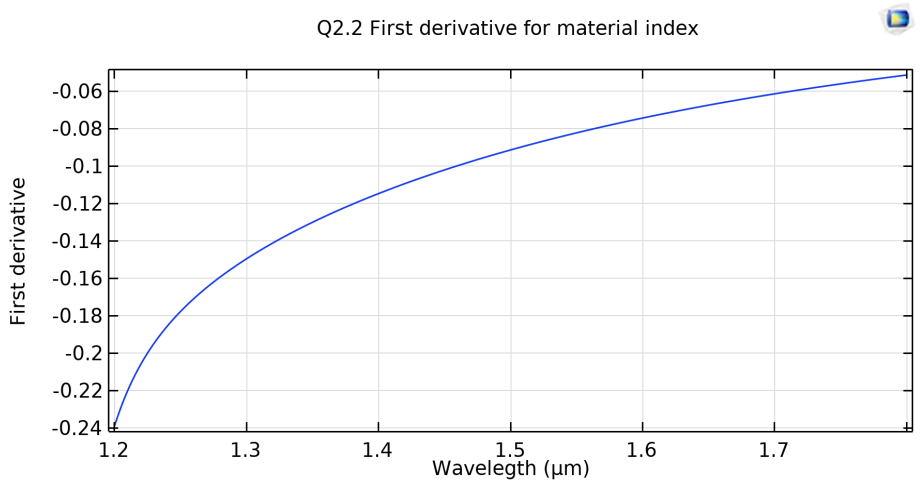

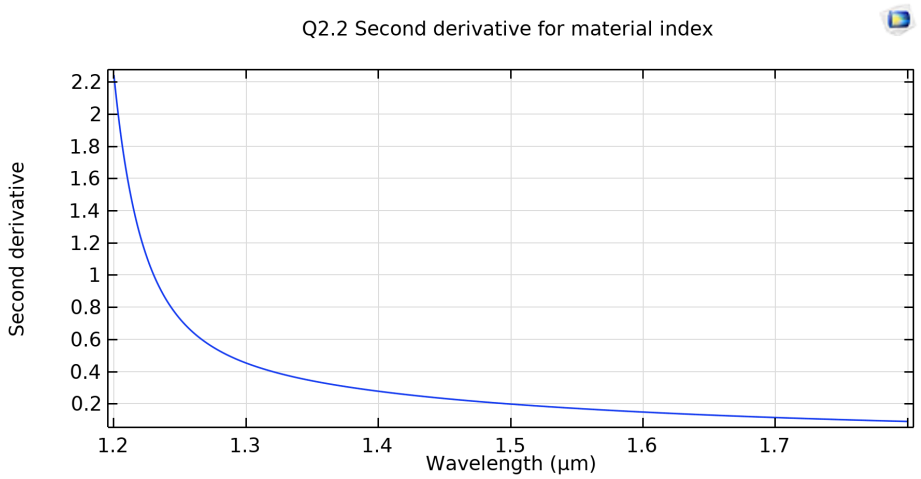

2.3 Repeat the same calculation for the mode effective refractive index neff (Hint: to calculate the mode index as a function of wavelength, make sure you run the simulation with varying silicon refractive index given in the Sellmeier equation above. This problem is asking, given the material dispersion of silicon(changing refractive index as a function of wavelength), how does the mode effective refractive index for the fundamental TE mode change?

Effective mode index for the fundamental TE mode decreases along with wavelength between 1200nm and 1800nm linearly.

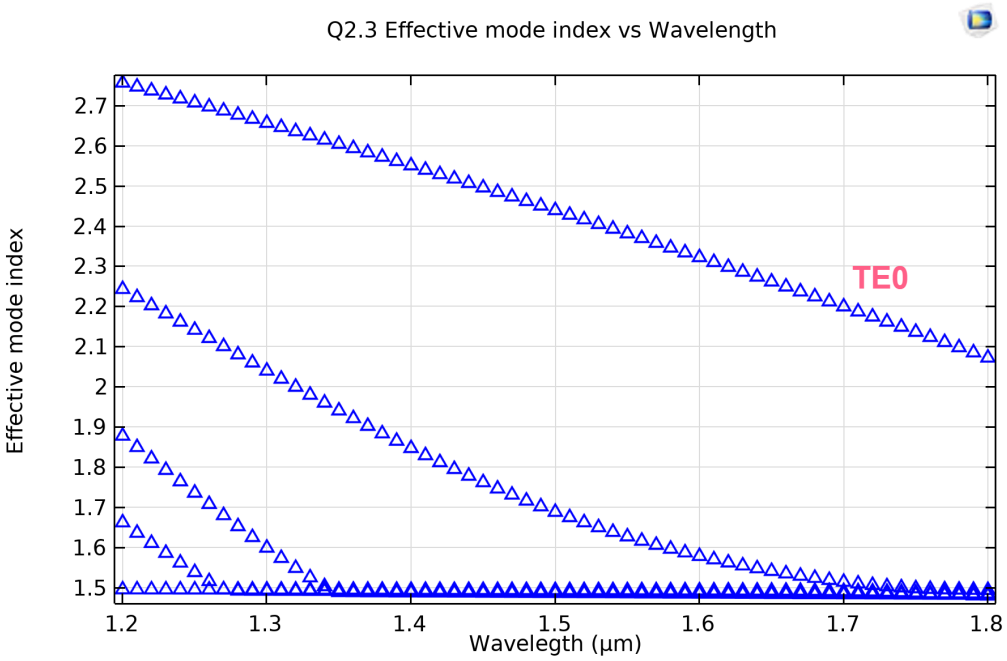

2.4 Calculate the effective mode area given by:

$$A_{eff} = \frac{(\int |E|^2)^2}{\int |E|^4}$$

Integration area is selected to be 8, 9, 11 and set up variable “area” to calculate the effective mode area.

Name	Expression
area	integral(abs(emw.Ez)^2)^2/int_core(abs(emw.Ez)^4)

Since the simulation results include too many non-physical modes. So, the bottom layer Silicon is replaced with SiO2.

After the modification of the simulation file, the effective mode area against wavelength is shown below. Due to long simulation time, only fundamental TE and TM modes, and some higher order modes data are plotted.

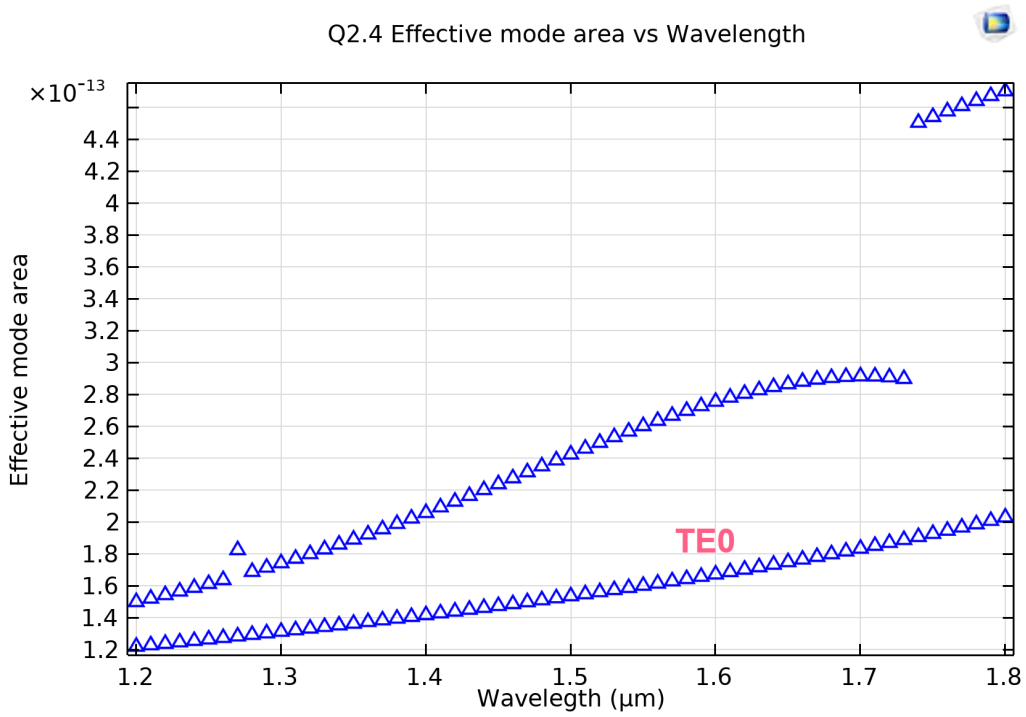

2.5 What is the ratio between the effective mode area and the geometrical area (cross-section of the waveguide)? The nonlinear coefficient scales as $\gamma = n_2\omega/(A_{eff}c)$ which is why nonlinear processes become significantly enhanced in nanoscale waveguides. Comment on the final result

Based on the calculated effective mode area in Q2.4. The data is taken to compare to geometric area (i.e. wvg_w*wvg_t).

The ratio between effective mode area and the geometrical area is:

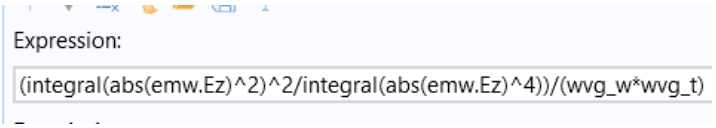

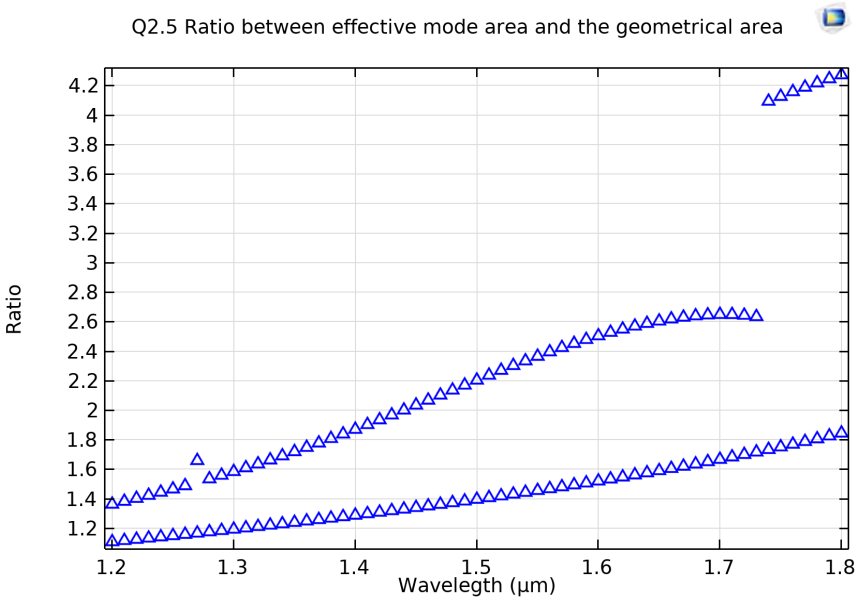

The simulated results tell us that the effective mode area is proportional to geometrical area. $\gamma \propto \frac{1}{A_{eff}}$. The smaller the A_{eff} , the larger the nonlinear coefficient. The simulated plot verified that nonlinear processes become significantly enhanced in nanoscale waveguides.

To avoid this nonlinear effect, large effective mode areas or large geometrical areas are suggested to be used in telecommunication systems, cryptographic systems, etc.

2.6 Suppose we want to study the degenerate four wave mixing process in this silicon waveguide with the pump wavelength fixed at 1550 nm. What are the wavelength(s) of the signal and idler photons produces in this process?
(Hint : you can ignore non-linear effects relating to the intensities of the pump, signal and idler)

Phase matching,

$$2\omega_p = \omega_s + \omega_i$$

$$\because \omega = nkc = n\frac{2\pi}{\lambda}c$$

$$\therefore \frac{2n_p}{\lambda_p} = \frac{n_s}{\lambda_s} + \frac{n_i}{\lambda_i} \text{ ———— (1)}$$

Energy,

$$E = hf$$

$$2hf_p = hf_s + hf_s$$

$$\frac{2n_p}{\lambda_p} = \frac{n_p}{\lambda_i} + \frac{n_p}{\lambda_s} \text{ ———— (2)}$$

The two formulas (1) and (2) deduced through phase matching and energy method matched.

According to the plot in Q2.1, although the line is non linear between 1200nm and 1800nm, to me, points near 1550nm on the TE0 line can be said to be the wavelengths of the signal and idler photons. I take 1540nm to be the wavelength of signal and 1560nm to be the wavelength of idler. Now go to COMSOL check the simulated results and substitute into the equation to verify.

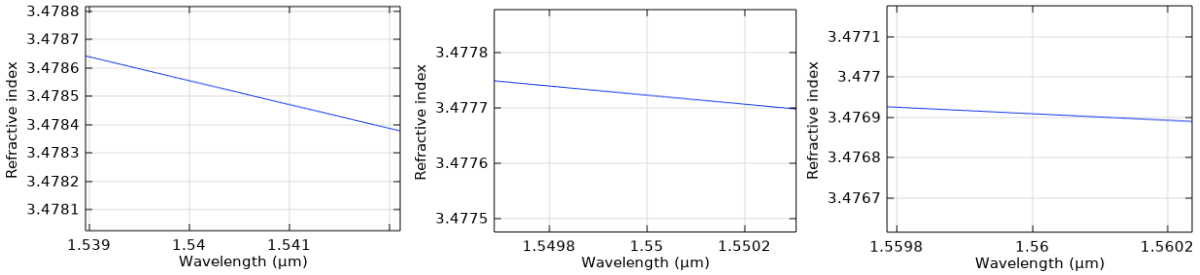

From COMSOL simulation, the effective mode index at 1540nm is 3.47855, at 1550nm is 3.47772 and at 1560 is 3.47691.

$$LHS = \frac{2n_p}{\lambda_p}$$

$$LHS = \frac{2(3.47772)}{1550nm}$$

$$LHS = 4487380.65$$

$$RHS = \frac{n_s}{\lambda_s} + \frac{n_i}{\lambda_i}$$

$$RHS = \frac{3.47855}{1540nm} + \frac{3.47691}{1560nm}$$

$$RHS = 4487587.16$$

LHS and RHS answers are extremely close within 0.005% difference.

∴ The statement that I suggest wavelength of signal and idler photons are 1540nm and 1560nm correspondingly, is valid.

Reference:

[1] Zhang, Z., Hu, X., & Wang, J. (2015). On-chip optical mode exchange using tapered directional coupler. In Scientific Reports (Vol. 5, Issue 1). Springer Science and Business Media LLC. https://doi.org/10.1038/srep16072

[2] Zhao, W., Liu, R., Peng, Y., Yi, X., Chen, H., & Dai, D. (2022). High-performance silicon polarization switch based on a Mach–Zehnder interferometer integrated with polarization-dependent mode converters. In Nanophotonics (Vol. 11, Issue 10, pp. 2293–2301). Walter de Gruyter GmbH. https://doi.org/10.1515/nanoph-2022-0022

[3] Heshmati, S., Taleb, H., & Rahmani, A. (2018). Complex Sellmeier equation for the refractive index of semiconductors in the opaque region. In Optik (Vol. 172, pp. 851–854). Elsevier BV. https://doi.org/10.1016/j.ijleo.2018.07.099

[4] Luke, S., Sudheer, S. K., & Pillai, V. P. M. (2015). Modeling and analysis of a highly birefringent chalcogenide photonic crystal fiber. In Optik (Vol. 126, Issue 23, pp. 3529–3532). Elsevier BV. https://doi.org/10.1016/j.ijleo.2015.08.190

[5] Wen, J., Liang, B., Sun, W., He, C., Xiong, K., Yu, H., Zhang, H., Wu, Z., & Wang, Q. (2024). Coherence analysis of supercontinuum generation in nitrobenzene liquid-core photonic crystal fiber based on adaptive step-size methods. In Optical and Quantum Electronics (Vol. 56, Issue 4). Springer Science and Business Media LLC. https://doi.org/10.1007/s11082-023-06267-6

[6] Zhao, W., Liu, R., Peng, Y., Yi, X., Chen, H., & Dai, D. (2022). High-performance silicon polarization switch based on a Mach–Zehnder interferometer integrated with polarization-dependent mode converters. In Nanophotonics (Vol. 11, Issue 10, pp. 2293–2301). Walter de Gruyter GmbH. https://doi.org/10.1515/nanoph-2022-0022

[7] Driscoll, J. B., Liu, X., Yasseri, S., Hsieh, I., Dadap, J. I., & Osgood, R. M. (2009). Large longitudinal electric fields (E_z) in silicon nanowire waveguides. In Optics Express (Vol. 17, Issue 4, p. 2797). Optica Publishing Group. https://doi.org/10.1364/oe.17.002797